Theoretical study of C20 fullerene dimerization: A facile [2+2] cycloaddition

ARTICLE *in* CHEMICAL PHYSICS LETTERS · JUNE 2002

Impact Factor: 1.9 · DOI: 10.1016/S0009-2614(02)00735-2

2 AUTHORS, INCLUDING:

Cheol Ho Choi
Kyungpook National University
111 PUBLICATIONS **2,123** CITATIONS

SEE PROFILE

27 June 2002

Chemical Physics Letters 359 (2002) 446–452

CHEMICAL PHYSICS LETTERS

www.elsevier.com/locate/cplett

Theoretical study of C_{20} fullerene dimerization: a facile [2+2] cycloaddition

Cheol Ho Choi [a,*], Hong-In Lee [b]

[a] *Department of Chemistry, College of Natural Sciences, Kyungpook National University, Taegu 702-701, Republic of Korea*
[b] *Department of Chemistry Education, Kyungpook National University, Taegu 702-701, Republic of Korea*

Received 14 February 2002; in final form 15 April 2002

Abstract

Dimerization of the C_{20} cage was studied with HF and DFT methods. Eight dimers were found. Of these, *open*-[2+2] isomer turned out to be the most stable dimer. [2+2] isomer is the second most stable due to the high ring strain of the C_{20} cage, in contrast to the case of C_{60} dimers where [2+2] isomer is more stable. The number of inter-fullerene bonds varies from 1 to 4 in the eight isomers. Asymmetric stepwise reaction channel leading to the *open*-[2+2] isomer with no net activation barrier was found, showing that it is both thermodynamically and kinetically favorable. © 2002 Elsevier Science B.V. All rights reserved.

1. Introduction

The C_{20} cage, the smallest fullerene possible, had been only a theoretical molecule [1,2] until recent anion-photoelectron spectroscopy [3] and first-principle calculation [4] showed its existence in vapor phase. In addition to its existence, the chemical reactivity of the C_{20} cage has been of interest. Molecular dynamics simulations showed that the cage can be chemisorbed on diamond $(1\,0\,0)$-2×1 and on silicon$(1\,0\,0)$-2×1 surfaces retaining its cage shape even after the chemisorptions [5,6]. Another theoretical study showed that the C_{20} cage can also form condensed phases in several dimensions and the most stable phase is a simple-cubic-like phase with a metallic property [7].

Recently, laser desorption and ionization in a time-of-flight mass spectrometer identified first time a series of $(C_{20})_k^+$ oligomers $(k = 1\text{–}13)$, formed by a coalescence of the C_{20} cages [8]. They proposed that the coalescence started with [2+2] cycloaddition of the C_{20} cages as seen in the C_{60} fullerene. The direct addition of two C=C double bonds constitutes the [2+2] cycloaddition (Fig. 1a), which is orbital symmetry forbidden, thus it requires high activation energy [9]. The C_{60} fullerenes can be coalesced and polymerized by the [2+2] cycloaddition (Fig. 1b) under extreme conditions [10–12]. Dimerization of C_{60} was also reported under cyanide ion catalysis [13]. These observations

* Corresponding author. Fax: +82-53-950-6330.
E-mail address: cchoi@knu.ac.kr (C.H. Choi).

0009-2614/02/$ - see front matter
PII: S0009-2614(02)00735-2

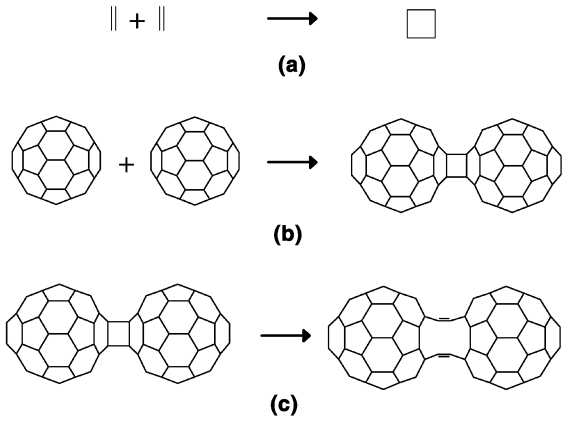

Fig. 1. (a) [2+2] Cycloaddition of two ethenes. (b) [2+2] Cycloaddition of two C_{60}'s. (c) Ring opening reaction or pericyclic reaction of C_{60} dimer.

indicate that the Woodward–Hoffmann rule is still valid in the [2+2] cycloaddition of C_{60} requiring high activation energy.

The coalescence mechanism of the C_{20} cage into larger oligomers and the type of the inter-fullerene bondings are however still uncertain. The C_{20} cage is more reactive than C_{60} due to its high ring strains. Therefore, somewhat different reaction behavior of the C_{20} cage is expected. In this paper, we study the possible isomers of the C_{20} cage dimers and their relative energetics in order to gain better understanding of the C_{20} cage reactivity and polymerization using ab initio and density functional methods. In addition, the reaction mechanism of the C_{20} cage dimerization, which would be the initial stage of the coalescence, is investigated to understand how the kinetics and thermodynamics interplay in the formation of the C_{20} cage oligomers.

2. Computational details

Hartree–Fock (HF) and density functional theory (DFT) with the B3LYP [14–16] exchange-correlation functional theories were adapted to compute the geometries and the energies. All electron basis sets, 6-31G(d) [17] were used throughout this work. To determine the minimum energy reaction path, the geometries of the minima and transition states were first optimized. Then, each stationary point was characterized by computing and diagonalizing the Hessian matrix (matrix of energy second derivatives). In order to follow the minimum energy path (MEP), the Gonzalez–Schlegel second-order method [18,19] was used with a step size of 0.3 $amu^{1/2}$-bohr. The general atomic and molecular electronic structure system (GAMESS) [20,21] program was employed for all of the computations. The reference energy, the energy of the C_{20} fullerene, was also calculated. Since the global minimum of the C_{20} dimer turned out to have D_{2h} symmetry [22], D_{2h} symmetry is imposed on the C_{20} cage in the geometry optimization.

3. Results and discussions

3.1. Products

Fully optimized structures and relative energetics of the C_{20} dimers are presented in Fig. 2 and Table 1. One would expect that the direct [2+2] cycloaddition, which would yield the [2+2] product, Fig. 2a, is the most stable isomer by analogy to the case of C_{60}, where the [2+2] structure, Fig. 1b, is the most stable. However, our calculation very interestingly showed that the *open*-[2+2] C_{20} dimer, Fig. 2b, is the most stable isomer of the C_{20} dimers. In the C_{60} dimers, the *open*-[2+2] structure, Fig. 1c, where the intra-fullerene bonds are broken and the inter-fullerene bonds have a double bond character as a result of a pericyclic reaction, is less stable by 70 kcal/mol than the [2+2] structure, Fig. 1b [23]. On the other hand, the *open*-[2+2] C_{20} dimer, Fig. 2b, is 36.6 kcal/mol more stable than the [2+2] C_{20} dimer, Fig. 2a, according to B3LYP/6-31G(d) calculation. The extra stabilization of the *open*-[2+2] C_{20} dimer may come from the relief of the ring strain by breaking the intra-bonds while C_{60} already has small ring strain. Therefore, if the intra-fullerene bonds of the C_{60} dimer are broken, ring strain would increase to disrupt π-conjugation network. The stabilization energy of the *open*-[2+2] C_{20} dimer, calculated by B3LYP/6-31G(d) theory, is 145.2 kcal/mol compared to the two separate C_{20} cages, indicating that a great deal of internal energy is released during the dimerization

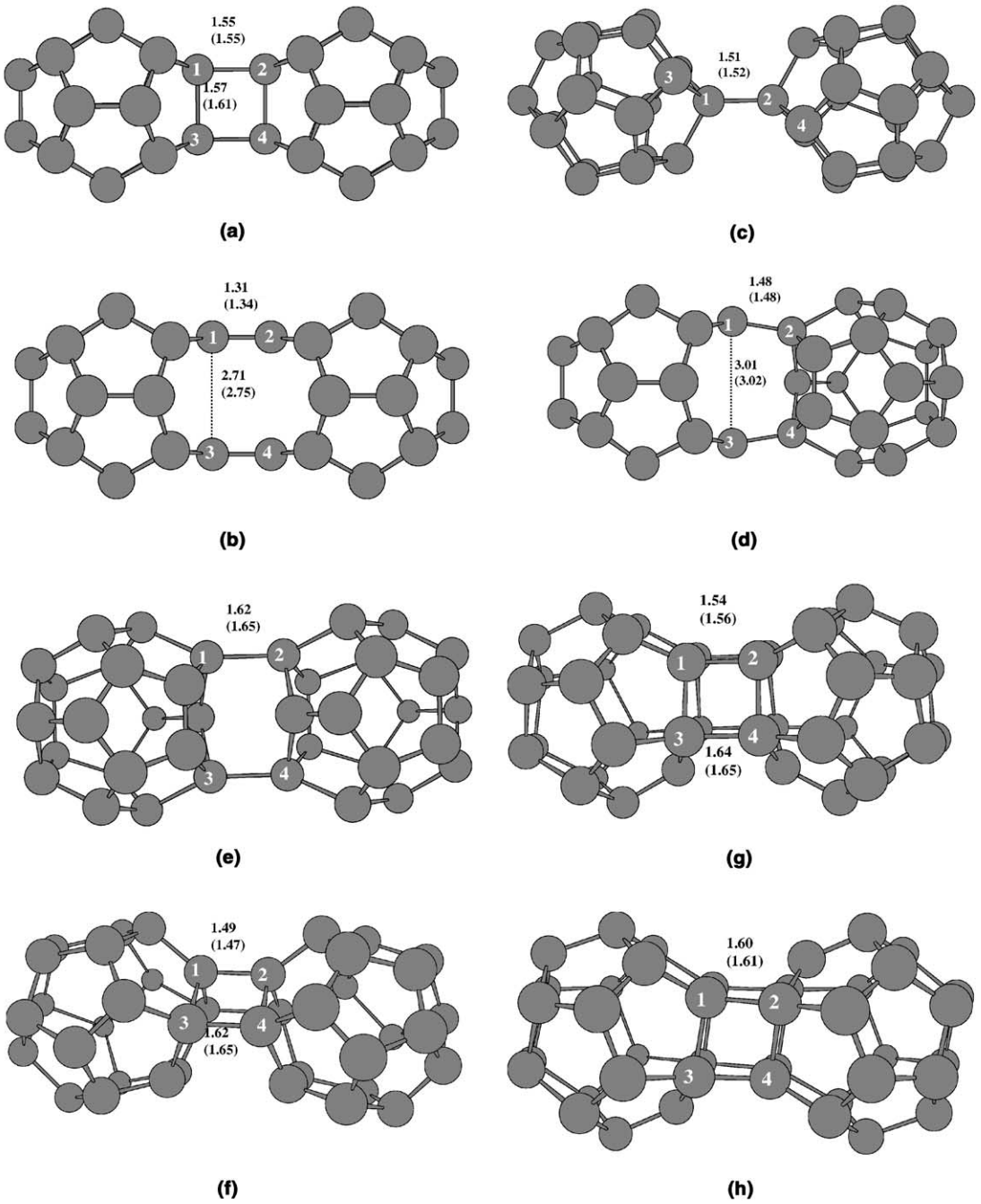

Fig. 2. (a) [2+2], (b) *open*-[2+2], (c) [1+1], (d) [5+2], (e) *di*-[5+5], (f) *tri*-[5+5], (g) *tetra*-[5+5], and (h) *tetra*-[4+4] isomers. The numbers and the numbers in parentheses are obtained with HF/6-31G(d) and B3LYP/6-31G(d) theories, respectively.

Table 1
Relative energies in kcal/mol among the possible isomers with respect to the two separate C_{20} cages

	open-[2+2]	[2+2]	[1+1]	[5+2]	*Di*-[5+5]	*Tri*-[5+5]	*Tetra*-[5+5]	*Tetra*-[4+4]
HF/6-31G(d)	−163.7	−136.9	−53.0	−44.5	−41.2	−67.2	−67.2	−35.4
B3LYP/6-31G(d)	−145.2	−108.6	−56.3	−52.9	−35.0	−54.0	−67.7	−24.4

followed by pericyclic reaction. The inter-fullerene bond length of Fig. 2b is calculated to be 1.34 Å indicating a double bond character, which is consistent with the above argument.

In addition to these two cycloaddition products, Figs. 2a and b, six more isomers were found. However, they are much less stable than the cycloaddition products. The [1+1] structure, Fig. 2c, where the two C_{20} cages are connected through C1–C2 bond, is the less stable than Fig. 2b by 88.9 kcal/mol in energy. The inter-fullerene bond shows a typical single bond length of 1.52 Å. Although it may not be an important isomer due to its high energy, it plays an important role in the formation of the [2+2] cycloaddition products as will be discussed in Section 3.2.

[5+2] isomer, Fig. 2d, where two edge carbon atoms in one C_{20} cage and two non-adjacent carbon atoms of a pentagon in another cage are connected, has two inter-fullerene bonds. Here, each number of the [5+2] nomenclature represents the number of carbon atoms in one cage, facing directly the other cage. The inter-fullerene bond (C1–C2) length is 1.48 Å showing a slightly shortened single bond. This shortening may be due to the extra electrons coming from the broken C1–C3 bond. This structure is less stable than the global minimum *open*-[2+2] structure by 92.3 kcal/mol in energy.

Di-[5+5] isomer, Fig. 2e, has also two inter-fullerene bonds while all intra-bonds are intact. The inter-fullerene bond length is 1.65 Å showing a slightly lengthened single bond, which may be due to the steric hindrance between the two pentagons facing each other. According to the B3LYP/6-31G(d) calculation, it is also less stable than the *open*-[2+2] structure by 110.2 kcal/mol.

Tri-[5+5] isomer, Fig. 2f, interestingly has three inter-fullerene bonds and is less stable than Fig. 2b by 91.2 kcal/mol. The two unique inter-fullerene bond lengths are 1.47 and 1.65 Å, respectively.

Tetra-[5+5] structure, Fig. 2g, has four inter-fullerene bonds, where four atoms out of five atoms in a pentagon are participating in the inter-fullerene interaction. It is less stable than Fig. 2b by 77.5 kcal/mol. The two unique inter-fullerene bond lengths are 1.56 and 1.65 Å, respectively.

Tetra-[4+4] structure, Fig. 2h, has also four inter-fullerene bonds, where the two facing pentagons are in an opposite way. The inter-fullerene bond length is 1.61 Å showing a slightly lengthened single bond. It is calculated to be more stable than two separate C_{20} cages by 24.4 kcal/mol making it the least stable isomer.

Any structure with more than four inter-fullerene bondings was not found. It is seen that the *open*-[2+2] and the [2+2] structures are thermodynamically much more favorable than the other isomers. However, thermodynamic stability alone would not guarantee their dominant populations in the reaction products. Kinetic activation barriers, therefore, need to be studied. The following section presents the possible reaction mechanisms yielding the cycloaddition products.

3.2. Reaction mechanisms of [2+2] and open-[2+2] products

As discussed in the introduction, the direct addition of two C_{20} cages may constitute [2+2] cycloaddition requiring a large activation barrier, if the reaction occurs through the concerted mechanism. However, no symmetric approach of the two cages was found by our calculation. Instead, low energy asymmetric reaction pathway was found by the study of potential energy surface using HF/6-31G(d) theory to locate transition states and intermediates. In that, the potential surface for the initial approach of the two C_{20} cage leading to the [1+1] product, Fig. 2c, does not show any activation barrier. Furthermore, the internal rotation with respect to the inter-fullerene bond (C1–C2) of

the [1+1] product exhibits extremely flat potential surface. For this reason, the [1+1] isomer would be better described as a meta-stable intermediate. By making a bond between C3 and C4 of Fig. 2c, the isomer becomes the [2+2] cycloaddition product, Fig. 2a. We were not able to locate any transition state that connects the meta-stable intermediate [1+1] and the [2+2] product. Instead, point by point constraint potential energy surface scan was carried out and the result is presented in Fig. 3. The full geometry optimizations were done at a fixed distance between atoms 3 and 4 in Fig. 2c. Although this surface may not be the lowest possible surface, the curve does not show any sign of a transition state along the entire potential surface connecting the [1+1] and the [2+2] isomers. Thus, this numerical calculation confirms the existence of barrierless reaction pathway that yields the [2+2] cycloaddition product. This reaction channel constitutes an asymmetric stepwise mechanism. This finding is unusual if we consider that the dimerization and polymerization of C_{60} requires rather harsh conditions. Therefore, the facile [2+2] cycloaddition in the dimerization of C_{20} is a direct representation of its high reactivity.

Although the [2+2] isomer is already very stable, it is not the global minimum. In order to obtain the global minimum, the *open*-[2+2] isomer, the two intra-fullerene bonds (C1–C3 and C2–C4 of Fig. 2a) of the [2+2] isomer must be broken. One could imagine either concerted or stepwise mechanism. The concerted mechanism requires a symmetric transition state where the two intra-fullerene bonds must be broken simultaneously while creating two inter-fullerene double bonds in a pericyclic fashion. On the other hand, in the stepwise mechanism, the two intra-fullerene bonds are broken one by one.

According to our search for transition states, only the stepwise mechanism was found. The transition states and the intermediate along this reaction channel are presented in Fig. 4. The

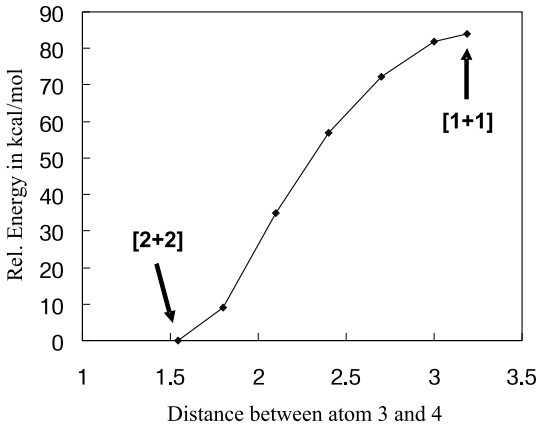

Fig. 3. Point by point constraint potential energy surface between the [2+2] and the [1+1] isomers obtained with HF/6-31G(d) theory. Abscissa represents the distance between C3–C4 of Fig. 2c.

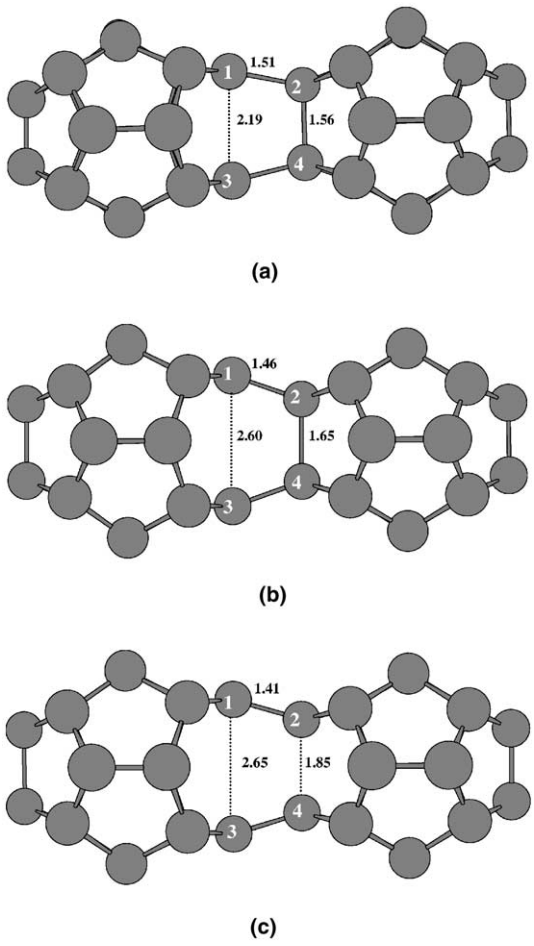

Fig. 4. (a) The structure of the transition state connecting the [2+2] isomer and the intermediate Fig. 4b. (b) Intermediate. (c) The transition state that connects Fig. 4b and the *open*-[2+2] isomer. The numbers are obtained with HF/6-31G(d) theory.

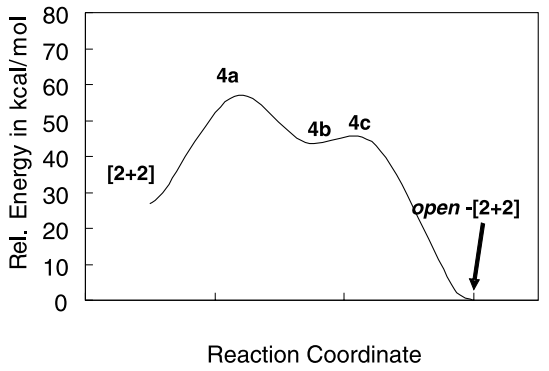

Fig. 5. Illustration of the potential energy surface that connects the [2+2] and the *open*-[2+2] isomers obtained with HF/6-31G(d) theory.

corresponding potential energy surface is illustrated in Fig. 5. Fig. 4a is the transition state connecting the [2+2] product, Fig. 2a, and the intermediate, Fig. 4b, with 30.0 kcal/mol of the forward activation energy. It should be noted, however, that the transition state Fig. 4a is still more stable than the two separate C_{20} cages by 106.93 kcal/mol. Therefore, this barrier is no more than an internal barrier which can be easily overcome. In Fig. 4a, one of the intra-fullerene bond is being broken with the bond length of 2.19 Å.

The intermediate Fig. 4b is less stable than the [2+2] isomer by 17.0 kcal/mol. In this structure, the other intra-bond (C2–C4) is somewhat elongated while the inter-fullerene bonds (C1–C2 and C3–C4) are shortened compared to those of the [2+2] isomer. The second transition state, Fig. 4c, where the remaining intra-fullerene bond (C2–C4) is being broken with the length of 1.85 Å, connects the intermediate Fig. 4b and the *open*-[2+2] isomer with a very small forward activation of 1.9 kcal/mol. Generally, HF overestimates the activation barrier of transition states. Therefore, the second transition state may be a HF artifact. Even if Fig. 4c does not exist, however, the general picture of the reaction channel would not be changed.

Overall it is seen that there is no net reaction barrier to the *open*-[2+2] structure indicating that it is both thermodynamically and kinetically favorable.

4. Conclusions

The dimerization reaction of the C_{20} cage was studied with the help of ab initio and density functional methods. Eight isomers of the C_{20} dimers were found. The number of the inter-fullerene bonds of the isomers varies from 1 to 4. Among these, the two theoretical methods consistently suggests that the *open*-[2+2] isomer, Fig. 2b, is the global minimum with large stabilization energy of 145.2 kcal/mol as compared to the two separate C_{20} cages. The second most stable isomer turned out to be the [2+2] product with the stabilization energy of 108.6 kcal/mol. The other isomers are much less stable than these two isomers.

Reaction channel that leads to the [2+2] and subsequently to the *open*-[2+2] cycloaddition products turned out to be a stepwise mechanism with no net activation barriers. Therefore, the global minimum, the *open*-[2+2] is both thermodynamically and kinetically favorable. As discussed in the introduction, recent experiment suggested [8] the [2+2] cycloaddition reactions as a possible coalescence mechanism. Current study further suggests that the *open*-[2+2] conformation is a likely candidate for the experimentally observed C_{20} fullerene dimerization.

Acknowledgements

This work was supported by Korea Research Foundation Grant (KRF-2001-003-D00056).

References

[1] P.R. Taylor, E. Bylaska, J.H. Weare, R. Kawai, Chem. Phys. Lett. 235 (1995) 558.
[2] J.C. Grossman, L. Mitas, K. Raghavachari, Phys. Rev. Lett. 75 (1995) 3870.
[3] H. Prinzbach, A. Weiler, P. Landenberger, F. Wahl, J. Worth, L.T. Scott, M. Gelmont, D. Olevano, B.v. Issendorff, Nature (London) 407 (2000) 60.
[4] M. Saito, Y. Miyamoto, Phys. Rev. Lett. 87 (2001) 035503.
[5] Z.Y. Man, Z.Y. Pan, Y.K. Ho, W.J. Zhu, Eur. Phys. J. D. 7 (1999) 595.
[6] A.J. Du, Z.Y. Pan, Y.K. Ho, Z. Huang, Z.X. Zhang, Y.X. Wang, Chem. Phys. Lett. 344 (2001) 270.

[7] Y. Miyamoto, M. Saito, Phys. Rev. B. 63 (2001) 161401.
[8] R. Ehlich, P. Landenberger, H. Prinzbach, J. Chem. Phys. 115 (2001) 5830.
[9] R.B. Woodward, R. Hoffmann, The Conservation of Orbital Symmetry, VCH, Weinheim, 1970.
[10] S. Pekker, L. Forro, L. Mihaly, A. Janossy, Solid State Commun. 90 (1994) 349.
[11] F. Cataldo, S. Progega, Polym. Int. 48 (1999) 143.
[12] V.A. Davydov, L.S. Kashevarova, A.V. Rakhmanina, V.M. Senyavin, R. Ceolin, H. Szwarc, H. Allouchi, V. Agafonov, Phys. Rev. B. 61 (2000) 11936.
[13] G. Wang, K. Komatsu, Y. Murata, M. Shiro, Nature 387 (1997) 583.
[14] A.D. Becke, J. Chem. Phys. 98 (1993) 5648.
[15] P.J. Stephens, F.J. Devlin, C.F. Chablowski, M.J. Frisch, J. Phys. Chem. 98 (1994) 11623.
[16] R.H. Hertwig, W. Koch, Chem. Phys. Lett. 268 (1997) 345.
[17] W.J. Hehre, R. Ditchfield, J.A. Pople, J. Chem. Phys. 56 (1972) 2257.
[18] C. Gonzalez, H.B. Schlegel, J. Phys. Chem. 94 (1990) 5523.
[19] C. Gonzalez, H.B. Schlegel, J. Chem. Phys. 95 (1991) 5853.
[20] M.W. Schmidt et al., J. Comput. Chem. 14 (1993) 1347.
[21] G.D. Fletcher, M.W. Schmidt, M.S. Gordon, Adv. Chem. Phys. 110 (1999) 267.
[22] S. Grimme, C. Muck-Lichtenfeld, Chem. Phys. Chem 2 (2002) 207.
[23] C.H. Choi, M. Kertesz, Chem. Phys. Lett. 282 (1998) 318.